

Cochlioquinone derivatives produced by coculture of endophytes, *Clonostachys rosea* and *Nectria pseudotrichia*

Ferry Ferdiansyah Sofian^a, Takuma Suzuki^b, Unang Supratman^c, Desi Harneti^c, Rani Maharani^c, Supriatno Salam^d, Fajar Fauzi Abdullah^e, Takuya Koseki^b, Kurumi Tanaka^f, Ken-ichi Kimura^{a,f}, Yoshihito Shiono^{a,b,*}

^a The United Graduate School of Agricultural Sciences, Iwate University, Morioka, Iwate 020-8550, Japan

^b Department of Food, Life, and Environmental Science, Faculty of Agriculture, Yamagata University, Tsuruoka, Yamagata 997-8555, Japan

^c Department of Chemistry, Faculty of Mathematics and Natural Sciences, Universitas Padjadjaran, Jatinangor 45363, Indonesia

^d Faculty of Pharmacy, Universitas Mulawarman, Samarinda 75123, Kalimantan Timur, Indonesia

^e Department of Chemistry, Faculty of Mathematics and Natural Sciences, Universitas Garut, Garut 44151, Indonesia

^f Graduate School of Arts and Sciences, Iwate University, Morioka, Iwate 020-8550, Japan

ARTICLE INFO

Keywords:

Nectrianolin

Endophyte

Cytotoxicity

Coculture

Furanocochlioquinone

Furanocochlioquinol

ABSTRACT

Three new meroterpenoid derivatives, furanocochlioquinol (1) and furanocochlioquinone (2), as well as nectrianolin D (3), together with two known biogenetically related compounds 4 and 5 were isolated from a mixed culture of two mangrove-derived fungi, *Clonostachys rosea* B5–2 and *Nectria pseudotrichia* B69–1. The structures of 1–3 were deduced based on the interpretation of HRMS and NMR data. Compounds 1–5 exhibited cytotoxicity against human promyelocytic leukemia (HL60) cells with IC₅₀ values ranging from 0.47 to 10.16 μM.

1. Introduction

Fungal endophytes of plants are widespread and important for host plant health [1]. The fungal endophytic communities differ between leaves, wood, and roots. Rich microbial communities in the host appear to be associated with the ecology of host plants and their defense mechanisms against pathogens and insect herbivory [2]. Several endophytic fungi are able to secrete secondary metabolites in host plants, which exhibit antifungal and/or antimicrobial activity at low concentrations. Secondary metabolites play an important role in host plants [3]. For example, an initial report proposed that the endophyte belonging to the genus *Xylariaceae* isolated from elm trees, secretes a toxic antilarval metabolite, which causes Dutch elm disease in the host [4].

Genomic analysis of natural product-producing microorganisms has revealed that the biosynthetic potential of the natural products exceeds the number of natural products isolated under standard laboratory growth conditions. Thus, many gene clusters that encode natural products may be silent under standard laboratory culture conditions. Activation of these gene clusters may reveal new molecular skeletons or

derivatives of known compounds.

Several methods have been developed to activate these cryptic gene clusters [5]. For example, our group, as well as others, investigated the OSMAC approach to activate cryptic clusters in order to stimulate the production of novel natural products by fungi [6]. When the fungus, *C. rosea* B5–2 was cultured on apple juice-supplemented solid rice media, significant changes occurred in its secondary metabolism, resulting in the production of four novel compounds [7]. Another promising approach for generating is the use of microorganism coculture, which facilitates fungus-fungus interspecies interactions. Over the past decade alone, the number of publications focused on coculturing microorganisms has increased, including several notable examples [8]. Coculture allows for communication and competition among the microorganisms, which may be crucial for the synthesis of natural products especially where dense microbial populations are encountered. Therefore, in order to discover novel natural products, we evaluated existing methods and began investigating potential interactions among endophytes that altered secondary metabolite production.

In our continuing search for novel bioactive compounds from fungal metabolites, we investigated the coculture fermentation of 50

* Corresponding author at: The United Graduate School of Agricultural Sciences, Iwate University, Morioka, Iwate 020-8550, Japan.

E-mail address: yshiono@tds1.tr.yamagata-u.ac.jp (Y. Shiono).

endophytic fungal strains that isolated from mangrove plants, together with their monoculture extract. After analyzing the HPLC profiles of the co-cultivation extracts, we found that the co-cultivation of *C. rosea* B5–2 with *N. pseudotrichia* B69–1 led to the production of different metabolites compared to those produced by cultivating each fungus individually. Here, we describe the isolation and structure elucidation of the new metabolites, as well as the cytotoxic activities of the isolated compounds.

2. Experimental

2.1. General experimental procedures

Optical rotations were measured with a Horiba SEPA-300 polarimeter, and UV and IR spectra were recorded with Shimadzu UV-1800 and Jasco J-20A (JASCO Co., Tokyo, Japan) spectrophotometers, respectively. Mass spectra were obtained with a Synapt G2. NMR spectra were recorded on a JEOL ECZ-600 at 600 MHz for ^1H and 150 MHz for ^{13}C . Chemical shifts are given on a δ (ppm) scale with TMS as an internal standard. ^1H , ^{13}C , COSY, HMQC and HMBC spectra were recorded using JEOL standard pulse sequences. Column chromatography was conducted on silica gel 60. TLC was carried out on Merck precoated silica gel 60 F₂₅₄ plates.

2.2. Fungal material and fermentation

The endophytes (B5–2 and B69–1 strains) were isolated from a surface sterilized branch of *Bruguiera gymnorrhiza* (L) Lamk, collected in a cost in Santolo Garut Beach, West-Java, Indonesia (southern latitude: 7°39'30"; eastern longitude: 107°41'19"). Fungal strains B5–2 and B69–1 were identified as *Clonostachys rosea* and *Nectria pseudotrichia*, respectively, by the using a DNA analysis of the 18S rDNA regions. They have been deposited at our laboratory in the Faculty of Agriculture of Yamagata. The fungi were precultured in Petri dishes (ϕ 90 × 15 mm) with 20 mL of medium composed of 0.2% potato extract, 1% glucose, and 1% agar in 1 L of deionized H₂O (PDA agar plates) at 25 °C for 10 days. Monoculture and coculture were separately performed under static conditions at 25 °C for 30 days in 1 L Erlenmeyers containing 100 g of the steamed unpolished rice and 150 mL of water.

2.3. Extraction and isolation

The moldy unpolished rice (1000 g) cocultured with *C. rosea* B5–2 with *N. pseudotrichia* B69–1, was extracted with methanol, and the methanol extract was concentrated. The resulting aqueous concentrate was partitioned into *n*-hexane (300 mL) and EtOAc (300 mL × 3) layers. The purification from the EtOAc layer was guided by the intense blue characteristic coloration with vanillin-sulfuric acid solution on TLC plates. The EtOAc layer (3.6 g) was chromatographed on a silica gel CC using first a stepwise of *n*-hexane/EtOAc (100:0:100, v/v; each 500 mL) and then a mixture of EtOAc/MeOH (50:50) as eluting solvents to give 12 fractions (Frs. 1–1–1–12). Frs. 1–4 and 1–5 (330 mg) were chromatographed on a silica gel CC using a stepwise gradient of CHCl₃/EtOAc (100:0–0:100, v/v; each 300 mL) to give 12 fractions (Frs. 2-1–2-12). Fr. 2–5 (126 mg) was subjected to ODS CC by eluting stepwise with H₂O and an increasing ratio of MeOH (100:0–0:100, v/v; each 100 mL) to afford 12 fractions (Frs. 2–5–1–2-5-11). Fr. 2–5–6 (70 mg) was purified by semi-preparative HPLC eluted with H₂O/MeOH (20:80) to yield **1** (3.7 mg) and **2** (3.0 mg). Frs. 1–6 and 1–7 (320 mg) were chromatographed on a silica gel CC using a stepwise gradient of CHCl₃/EtOAc (100,0–0:100, v/v; each 300 mL) to give 12 fractions (Frs. 3-1–3-12). Fr. 3–4 (100 mg) was subjected to ODS CC by eluting stepwise with H₂O and an increasing ratio of MeOH (100:0–0:100, v/v; each 100 mL) to afford 11 fractions (Frs. 3-4-1–3-4-11). Fr. 3-4-8 (50 mg) was subjected to flash silica gel CC (*n*-hexane/EtOAc, 5:1) to afford **3** (5.0 mg) and **4** (5.0 mg). Fr. 1–7 (240 mg) was chromatographed on silica gel CC using a stepwise

Table 1

^1H (600 MHz) and ^{13}C NMR (150 MHz) spectroscopic data of furanocochloquinol (**1**) and furanocochloquinone (**2**) in CDCl₃.

Pos.	1		2	
	δ_{C} , type	δ_{H} , (<i>J</i> in Hz)	δ_{C} , type	δ_{H} , (<i>J</i> in Hz)
1	13.9, CH ₃	1.81, d (7.2)	14.2, CH ₃	1.83, d (6.6)
2	126.4, CH	6.04, q (7.2)	127.8, CH	6.00, q (6.6)
3	127.7, C		125.7, C	
4	155.2, C		156.7, C	
5	109.8, C		116.6, C	
6	132.3, C		123.6, C	
7	136.7, C		150.4, C	
8	136.5, C		153.2, C	
9	108.2, C		109.7, C	
10	147.4, C		176.9, C	
11	96.0, CH	6.35, s	176.2, C	
12	113.7, CH	6.59, s	111.8, CH	6.34, s
13	142.7, C		140.3, C	
14	78.0, C		83.3, C	
15	38.1, CH ₂	2.09, m 2.24, td (13.8, 3.0)	37.8, CH ₂	2.03, m 2.29, dt (13.2, 3.6)
16	24.8, CH ₂	1.62–1.72*	24.6, CH ₂	1.71, m 1.82, m
17	81.8, CH	3.19, br.d (10.0)	81.3, CH	3.19, m
18	38.1, C		38.3, C	
19	35.0, CH ₂	1.60, m 2.11, m	34.9, CH ₂	1.56, m 2.10, m
20	21.9, CH ₂	1.52, m 1.62–1.72*	21.8, CH ₂	1.56, m 1.70, m
21	84.4, CH	3.16, dd (10.8, 2.4)	84.7, CH	3.18, m
22	72.4, C		71.9, C	
23	23.7, CH ₃	1.18, s	23.8, CH ₃	1.17, s
24	26.1, CH ₃	1.19, s	26.1, CH ₃	1.18, s
25	20.9, CH ₃	1.17, s	20.1, CH ₃	1.09, s
26	26.6, CH ₃	1.47, s	27.6, CH ₃	1.59, s
27	9.7, CH ₃	2.15, s	10.3, CH ₃	2.32, s
28	14.5, CH ₃	2.09, s	14.0, CH ₃	2.01, s

* Overlapped signals.

gradient of CHCl₃–EtOAc to give 11 fractions (Frs. 4-1 - 4-11). Frs. 4–7 and 4–8 (75 mg) were subjected to ODS CC by eluting stepwise with H₂O and an increasing ratio of MeOH to afford crude compound **5**, which was finally purified by flash silica gel CC (CHCl₃/MeOH, 50:1) to afford **5** (6.0 mg).

Table 2

^1H (600 MHz) and ^{13}C NMR (150 MHz) spectroscopic data of nectrianolin D (**3**) in CDCl₃.

Pos.	3	
	δ_{C} , type	δ_{H} , mult. (<i>J</i> in Hz)
1	136.6, C	
2	127.4, C	
3	32.8, CH ₂	1.85, t (6.0)
4	19.5, CH ₂	1.50, m
5	39.8, CH ₂	1.37, m
6	35.0, C	
7	27.4, CH ₂	2.04, t (11.4)
8	40.3, CH ₂	2.04, t (11.4)
9	144.2, C	
10	119.7, CH	5.20, d (8.4)
11	65.9, CH	4.83, d (8.4)
12	19.9, CH ₃	1.54, s
13	28.7, CH ₃	0.93, s
14	28.7, CH ₃	0.94, s
15	17.0, CH ₃	1.73, s
1'	195.6, C	
2'	121.4, CH	5.96, s
3'	158.8, C	
4'	63.1, CH	4.46, br.s
5'	60.9, CH	3.67, br.s
6'	60.5, C	
7'	62.5, CH ₂	4.18, d (17.4) 4.40, d (17.4)

2.3.1. Furanocochliquinol (1)

Amorphous powder; $[\alpha]_D^{20} + 110^\circ$ (c 0.2, MeOH); UV (MeOH): λ_{\max} (log ϵ): 242 (4.7), 324 (4.0); IR (KBr): 3334, 2945, 1640, 1600, 1455, 1014 cm^{-1} ; ECD (MeOH) λ_{\max} ($\Delta\epsilon$) 259 (−18.0), 319 (14.1) nm; ^1H NMR (600 MHz, CDCl_3) and ^{13}C NMR (150 MHz, CDCl_3) data, see Table 1; HRESITOFMS (positive ion mode) m/z 453.2649 ($[\text{M} + \text{H}]^+$, calcd for $\text{C}_{28}\text{H}_{37}\text{O}_5$, 453.2640).

2.3.2. Furanocochliquinone (2)

Amorphous powder; $[\alpha]_D^{20} + 80^\circ$ (c 0.10, MeOH); UV (MeOH): λ_{\max} (log ϵ): 222 (4.3), 300 (4.1); IR (KBr): 3404, 2935, 1704, 1292, 1014 cm^{-1} ; ECD (MeOH) λ_{\max} ($\Delta\epsilon$) 213 (−5.3), 250 (11), 297 (−2.3), 328 (6.4), 380 (7.5) nm; ^1H NMR (600 MHz, CDCl_3) and ^{13}C NMR (150 MHz, CDCl_3) data, see Table 1; HRESITOFMS (positive ion mode) m/z 467.2433 ($[\text{M} + \text{H}]^+$, calcd for $\text{C}_{28}\text{H}_{35}\text{O}_6$, 467.2430).

2.3.3. Nectrianolin D (3)

Amorphous powder; $[\alpha]_D^{20} - 88^\circ$ (c 0.68, MeOH); UV (MeOH): λ_{\max} (log ϵ): 206 (4.3), 242 sh (3.9); IR (KBr): 3400, 2935, 1678, 1252, 1044, 740 cm^{-1} ; ECD (MeOH) λ_{\max} ($\Delta\epsilon$) 246 (−6.0), 338 (−3.0) nm; ^1H NMR (600 MHz, CDCl_3) and ^{13}C NMR (150 MHz, CDCl_3) data, see Table 2; HRESITOFMS (positive ion mode) m/z 399.2152 ($[\text{M} + \text{Na}]^+$, calcd for $\text{C}_{22}\text{H}_{32}\text{NaO}_5$, 399.2147).

2.4. ECD calculations

In order to clarify the absolute configurations of **1**, **2**, and **3**, computational methods were utilized. The DFT and TDDFT calculations were carried out in the gas phase with Gaussian 09 software [9]. The conformational analysis was initially performed using the GMMX program [10] with the MMFF94 force field. The selected conformer was optimized at B3LYP/6-31G(d) using DFT. The ECD calculations were conducted using the TDDFT method for 30 excited states at the B3LYP/6-311G(d) level in the gas phase. The CD spectra were generated by the program SpecDis using a Gaussian band shape with 0.3 eV.

2.5. Calculated ^{13}C NMR data of 2

Conformational analyses were performed by random searching with an energy cutoff of 3.5 kcal/mol using the GMMX program software [10]. The MMFF94S force field was employed. The conformers were reoptimized in the gas phase at the DFT/B3LYP/6-31G(d) level using the Gaussian 09 program. The ^{13}C NMR shielding constants of **3** were calculated by the GIAO method at the $\omega\text{B97X-D}/6-311\text{G(d)}$ level of theory in CHCl_3 . The computational ^{13}C NMR data were obtained by linear regression. The ^{13}C NMR chemical shift of tetramethylsilane was calculated at the same level and used as reference. The calculated NMR data of these conformers were averaged according to the Boltzmann distribution theory. Boltzmann distributions were estimated from the B3LYP and the $\omega\text{B97X-D}$ energies. The linear correlation coefficient (R^2) and MAE were calculated for evaluation of the deviations between the experimental and calculated results.

2.6. Cell culture and cytotoxicity assay

HL60 cells (RCB0041, RIKEN BioResource Center, Tsukuba, Japan) was grown in RPMI 1640 medium supplemented with 10% heat-inactivated FBS (Sigma-Aldrich Corp., St. Louis, USA) and penicillin (50 units/mL)-streptomycin (50 $\mu\text{g}/\text{mL}$) (Gibco Corp., Carlsbad, USA) in a humidified atmosphere at 37 $^\circ\text{C}$ under 5% CO_2 . All isolated compounds were examined for cytotoxicity activity by MTT assay using published protocol [11].

3. Results and discussion

Two endophytic fungi, *C. rosea* B5–2 and *N. pseudotrichia* B69–1

isolated from the mangrove plant, *B. gymnorhiza* (L.) Lamk, were cultured on PDA agar plates. The fungi were streaked apart on the left and right sides of the agar plate and cultured for 10 days. A brown pigment appeared at the contact surface of the coculture (Fig. S1). This indicated that a cryptic gene cluster may have been activated by the contact of both fungi, generating this brown pigment.

Fractionation and purification of the EtOAc extract of the *C. rosea* B5–2 and *N. pseudotrichia* B69–1 coculture by HPLC afforded 3 new meroterpenoids, **1**, **2**, and **3** as well as two known compounds **4** and **5**. The two known compounds were identified as 12-dehydrocochliquinone D (necatripenoid B) (**4**) [12] and cochliquinone D (**5**) [13,14].

Compound **1** has the molecular formula $\text{C}_{28}\text{H}_{36}\text{O}_5$ as established by HRESITOFMS. Its UV spectrum shows an absorption maximum at 242 and 324 nm, which suggests the presence of a conjugated benzene chromophore. The IR absorptions suggested the presence of hydroxy (3334 and 2945 cm^{-1}) and benzene (1640 and 1600 cm^{-1}) groups in the structure. The ^{13}C NMR spectrum revealed 28 carbons (Table 1) that were classified by DEPT spectra analysis, which indicated that there were 7 methyls, 4 methylenes, 5 methines, and 12 quaternary carbons. This classification agrees with the molecular formula of **1**. The chemical formula of **1** requires 11 rings or unsaturation equivalents. Since 6 out of the 11 unsaturation equivalents are accounted for by the ^{13}C NMR data, it is inferred that a molecule of **1** contains five rings. The ^1H NMR spectrum (Table 1) of **1** displayed four quaternary methyls [δ_{H} 1.17 (3H, s, Me-25), 1.18 (3H, s, Me-23), 1.19 (3H, s, Me-24), 1.47 (3H, s, Me-26)], three olefinic methyls [δ_{H} 1.81 (3H, d, $J = 7.2$ Hz, Me-1), 2.09 (3H, s, Me-28), 2.15 (3H, s, Me-27)], two oxygenated methines [δ_{H} 3.16 (dd, $J = 10.8, 2.4$ Hz, H-21), 3.19 (1H, br.d, $J = 10$ Hz, H-17)], three olefinic protons [δ_{H} 6.04 (1H, q, $J = 7.2$ Hz, H-2), 6.35 (1H, s, H-11), 6.59 (1H, s, H-12)], and four methylene protons [δ_{H} 1.52 (1H, m, H-20), 1.60 (1H, m, H-19), 1.62–1.72 (H-16, 20), 2.09 (1H, m, H-15), 2.11 (1H, m, H-19), 2.24, (1H, td, $J = 13.8, 3.0$ Hz, H-15)]. Detailed analyses of the ^1H – ^1H COSY spectrum disclosed the presence of a partial structure shown as a bold line in Fig. 2. The ^1H and ^{13}C NMR spectroscopic data of **1** were very similar to those of **4**. The difference between the NMR spectra of **1** and **4** was the absence of a 1,4-benzoquinone group in **1** that was observed in **4** and the appearance of characteristic signals in **1** due to an 8H-furo[3,2-*h*][1]benzopyran moiety [δ_{C} 78.0 (C-14), 96.0 (C-11), 108.2 (C-9) 109.8 (C-5), 113.7 (C-12), 132.3 (C-6), 136.5 (C-8), 136.7 (C-7), 142.7 (C-13), 147.4 (C-10), 155.2 (C-4)]. The 8H-furo[3,2-*h*][1]benzopyran moiety was confirmed by the HMBC correlations (Fig. 2). In addition, HMBC correlations from Me-28 to C-4, and Me-1 to C-3, indicated that the *cis*-2-butene moiety was connected to C-4. The observed NOE correlations from H-25 to H-26, and from H-25 to H-12 and H-19 implied that Me-25 and Me-26 were cofacial (Fig. 3). The configurations at C-17 and C-21 were considered to be opposite face because protons at C-17 and C-21 in **1** had chemical shifts and coupling constants similar to those of **4** and **5**. In order to determine the absolute configuration of **1**, the calculated ECD spectrum of **1** was performed using time-dependent density functional theory (TDDFT) methodology. This analysis revealed that the calculated spectrum of **1** at the B3LYP/6-311G(d)//B3LYP/6-31G(d) level showed excellent agreement with the experimental ECD curve (Fig. 4A), which undoubtedly established the absolute configuration of **1**. Accordingly, the structure of **1** was referred to as furanocochliquinol.

The molecular formula of compound **2** was determined as $\text{C}_{28}\text{H}_{34}\text{O}_6$ from HRESITOFMS analysis, which indicated 12 degrees of unsaturation. The ^1H and ^{13}C NMR data of **2** (Table 1) were similar to that of **1**. In the ^1H NMR spectrum of **2**, methyl signals at δ_{H} 1.09, 1.17, 1.18, and 1.59 were assigned to Me-23, Me-24, Me-25, and Me-26, respectively. These signals, together with signals at δ_{H} 3.19 (H-17), and 3.18 (H-21) supported the presence of a methylated octahydrophenanthrene skeleton moiety. In addition, a methine proton signal at δ_{H} 6.35 (H-11) observed in **1** was absent in the ^1H NMR data of compound **2**, and in compound **2** a signal assigned to a ketone group was observed at δ_{C} 176.2 (C-11) by ^{13}C NMR. In order to establish the planar structure,

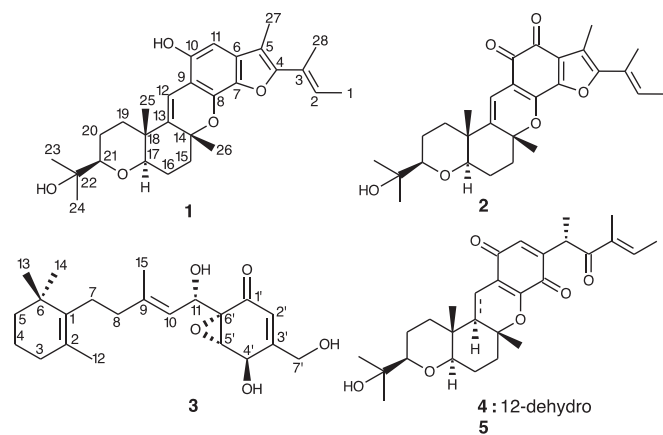


Fig. 1. Structures of compounds 1–5.

HMBC experiments were conducted on **2** (Fig. 2). HMBC correlations revealed two possible structures: a 1,2-quinone-type (**2**) or a 1,4-quinone-type (**2a**, Fig. S24). Discrimination between these two possibilities (**2** and **2a**) was achieved using theoretical NMR calculations. The experimental carbon resonances of **2** matched the calculated data for **2** with a correlation coefficient $R^2 = 0.9994$ (Fig. S24) and smaller $\Delta\delta_C$ values (Fig. 5) than those for **2a**, which had a $R^2 = 0.9984$ (Fig. S24). The presence of the ortho-benzoquinone ring system was supported by the ^{13}C NMR data of obionin A [15]. These results indicated that the 1,4-quinone-type **2a** could be clearly excluded. The relative configuration of **2** was identical to that of **1** based on the NOE experiments (Fig. 3). In order to define the absolute configuration of **2**, the calculated ECD spectrum of **2** obtained at the B3LYP/6-311G(d)//B3LYP/6-31G(d) level was compared with the experimental ECD curve (Fig. 4B) and confirmed the absolute configuration of **2**. Thus, compound **2** was referred to as furanocochloquinone.

The molecular formula of compound **3** was determined to be $\text{C}_{22}\text{H}_{32}\text{O}_5$ by HRESITOFMS data, which revealed seven degrees of unsaturation. The IR spectrum of **3** revealed the presence of hydroxyl and carbonyl groups. The UV spectrum of **3** indicated the presence of a conjugated enone. The ^{13}C NMR (Table 2) and DEPT spectra of **3** revealed carbon signals due to four methyl carbons, six methylene carbons, five methine moieties, and seven quaternary carbons, one of which was a carbonyl group. The aforementioned data suggested that **3** had three rings. The ^1H NMR of **3** (Table 2) showed signals due to four singlet methyl groups [δ_{H} 0.93 (s, Me-13), 0.94 (s, Me-14), 1.54 (s, Me-12), 1.73 (s, Me-15)], three oxygenated methine protons [δ_{H} 3.67 (br.s, H-5'), 4.46 (br.s, H-4'), 4.83 (d, $J = 8.4$ Hz, H-11)], a primary alcohol [δ_{H} 4.18 (d, $J = 17.4$ Hz, H-7'), 4.40 (d, $J = 17.4$ Hz, H-7'')], and two olefinic protons [δ_{H} 5.20 (d, $J = 8.4$ Hz, H-10), 5.96 (s, H-2')]. The ^1H – ^1H COSY spectrum of **3** demonstrated that **3** contained the partial structures represented by thick lines in Fig. 2. The connectivity of these fragments was determined by HMBC (Fig. 2). The double bond position was assigned by HMBC correlations from the olefinic methyl (Me-12) to two sp^2 carbons at δ_{C} 136.6 (C-1) and 127.4 (C-2) and to the methylene carbon at δ_{C} 32.8 (C-3). Additional HMBC correlations from Me-13 and Me-14 to C-1, C-5, and C-6, confirmed that the structure of **3** contained a trimethyl cyclohexene moiety (Fig. 2). The presence of a 3-methyl-2-penten-1-ol moiety was clarified using HMBC correlations from Me-15 to C-8, C-9, and C-10, and from H-11 to C-9 and C-10. The HMBC correlations from H-7 to C-2 and C-6 indicated that the pentenol moiety was located at C-1. Further HMBC analysis of **3** revealed correlations from H-2' to C-1', C-4', C-6', and C-7', and H-5' to C-1'. These data suggested the presence of an oxygenated cyclohexenone nucleus as well as hydroxymethyl and hydroxyl moieties. The planar structure of **3** was deduced from these results and is shown in Fig. 2. The relative configuration of **3** was determined on the basis of ^{13}C NMR shifts compared to the reported

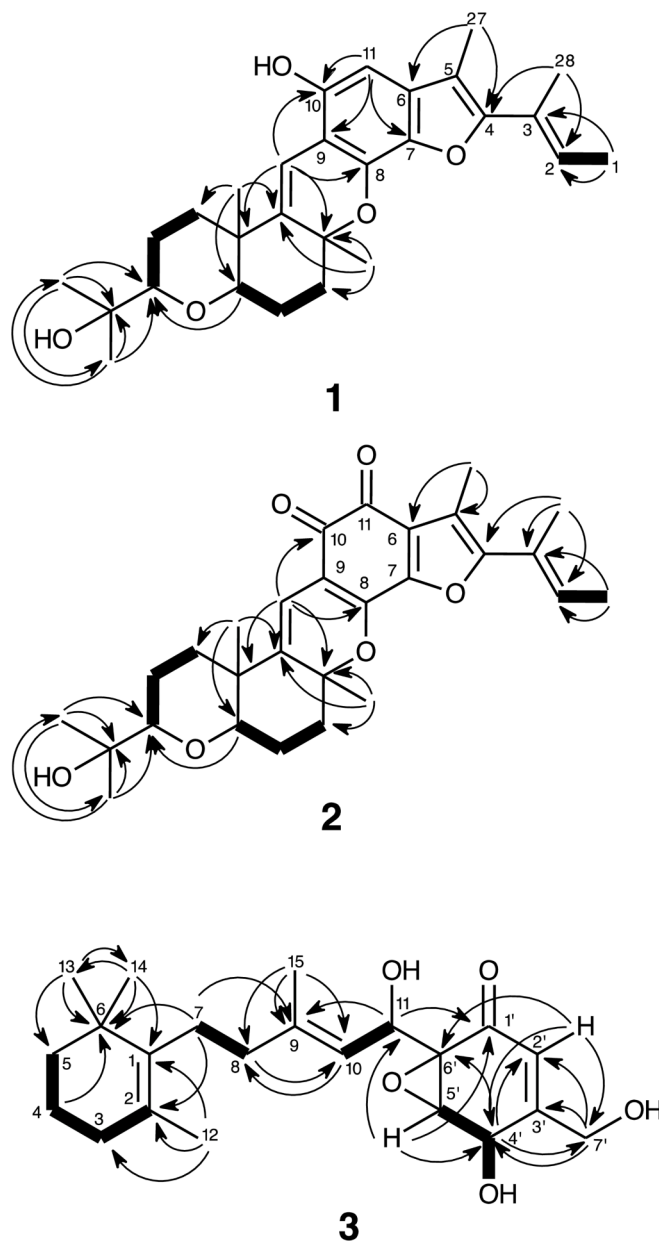


Fig. 2. Key COSY (bolds) and HMBC (arrows) correlations of compounds 1–3.

compounds and NOE (Fig. 3). The NOE correlation between H-8 and H-10 indicated an *E*-form double bond at C-9 and C-10. The *trans* orientation for both the epoxide and 4'-OH groups were assigned on the basis of their H-4' and H-5' 3J coupling constant of 0 Hz. The CD spectrum of **3** generated negative Cotton effects at 246 nm (-6.0) and 338 nm (-3.0). The CD data was compared with that of nectrianolin A [(4*R*,5*S*,6*S*)] [CD (MeOH) $\Delta\epsilon$: 248 (-4.2), 333 (-2.2) nm] [16]. This comparison suggested that the absolute configuration of **3** was (4*R*,5*S*,6*S*). In addition, in order to confirm the absolute configuration of **3** at C-4', C-5', and C-6' we compared the calculated ECD and the experimental ECD data of **3** (Fig. 4C). As for the relative configurations of the stereogenic center of the polyketide side chain, the *a*-orientation of 11-OH was assigned based on the NOE correlation of H-5'/H-10. This assignment was supported by conformational analysis conducted with density functional theory (DFT) calculations (B3LYP/6-311G(d) // B3LYP/6-31G(d)). Comparison of the dominant conformers of the two stereoisomers (11*S**,4'*R**,5'*S**,6'*S*')-**3** and (11*R**,4'*R**,5'*S**,6'*S*')-**3a**, only **3** could account for the NOE (H-5' and H-10) information (Fig. 6). Therefore, the

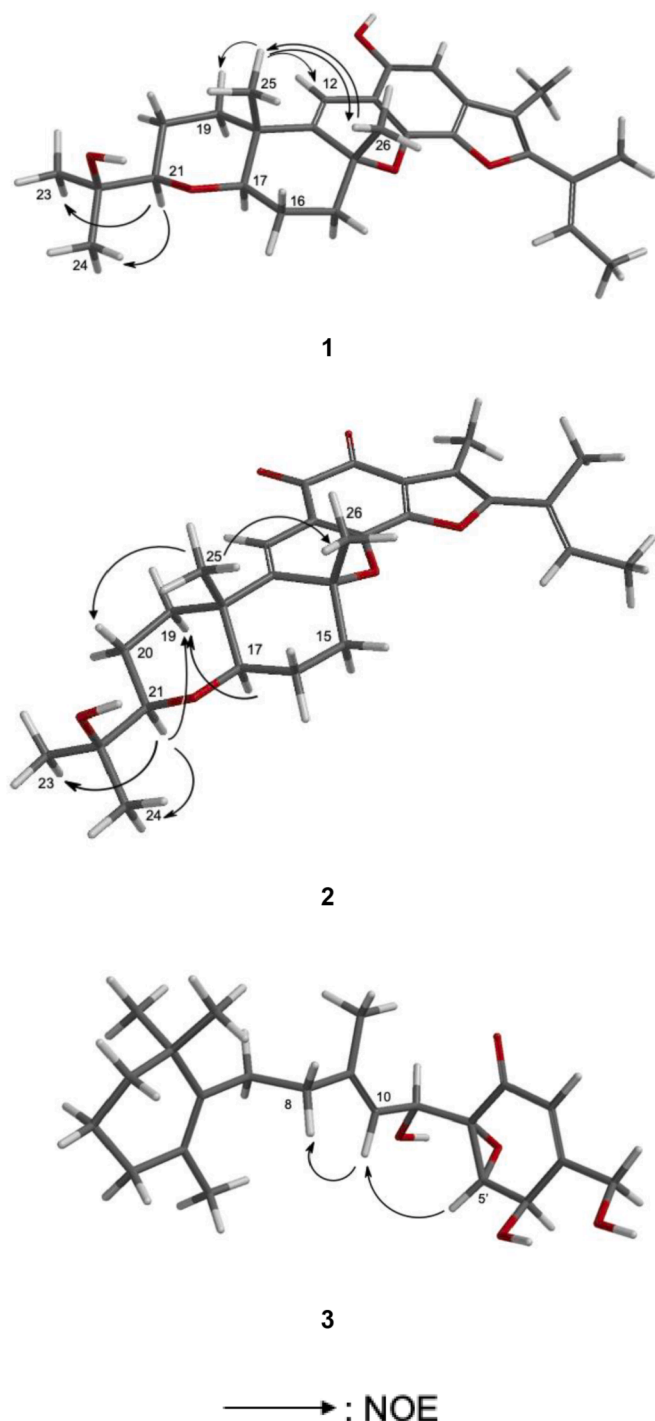


Fig. 3. Key NOE correlations of 1–3.

structure of **3** was established as shown in Fig. 1 and was referred to as nectrianolin D.

The biosynthetic pathways of **1**, **2**, **3**, **4** and **5** were proposed as shown in Scheme 1. Cyclization from an intermediate A to form the furan ring would lead to **1**. Cochlioquinone analogues oxygenated at C-11 such as arthropenoid D and cochlioquinone J were isolated from *Arthrinium* sp. NF2194 [12] and *Lycium barbarum* [17], respectively. Thus we proposed that compound **2** was thought to arise via hydroxylation at C-11 of **4**, and the subsequent nucleophilic attack of the hydroxyl group at C-7 to keto moiety at C-4 in the intermediate B (keto moiety at C-11) with the loss of a H₂O for the formation of furan ring.

The cytotoxicity of compounds **1**–**5** was evaluated using HL60 cells

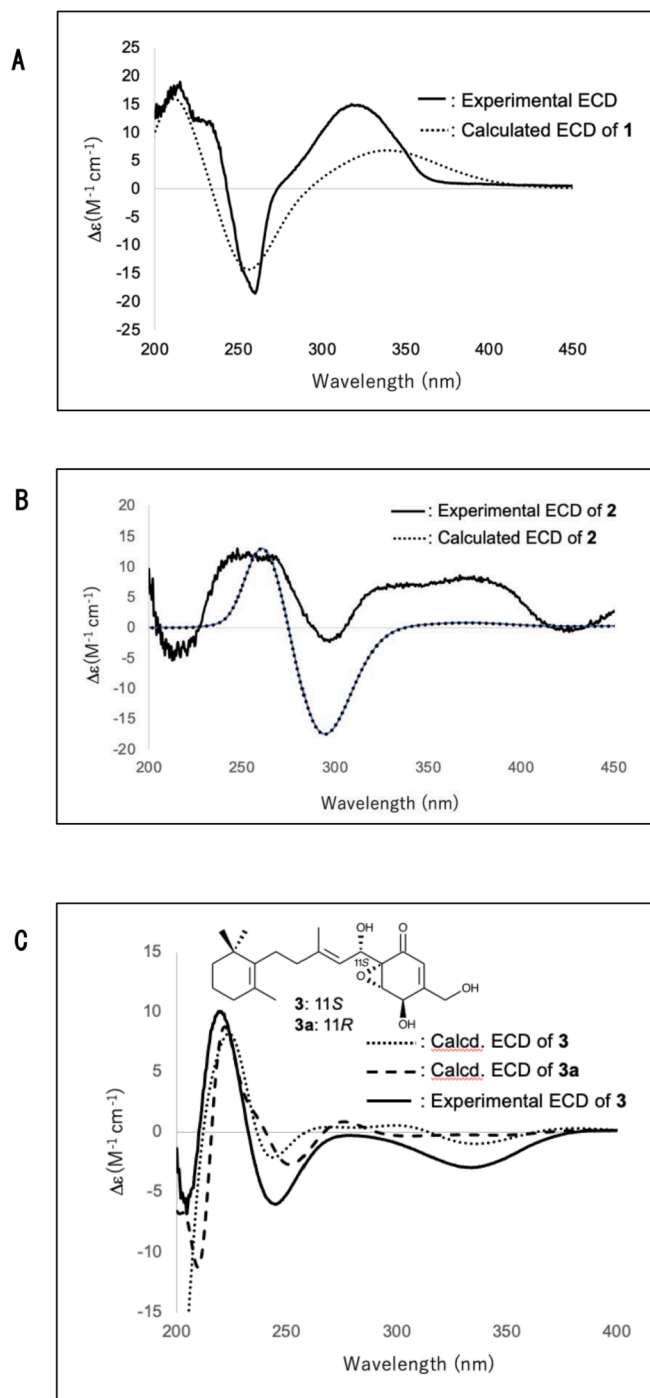


Fig. 4. Calculated and experimental ECD spectra of 1–3.

with camptothecin as a positive control (Table 3). Compounds **4** and **5** exhibited inhibitory activities with IC₅₀ values of 0.93 and 1.61 μM, respectively, implying that the dehydrogenation between C-12 and C-13 might contribute to this activity. Previous reports of the biological activity of cochlioquinone derivatives also indicated that the Δ¹²⁽¹³⁾ double bond was important for conferring the cytotoxic activities [18]. Comparison of compounds **1** and **2** to **4** revealed that the introduction of a furan ring increased their cytotoxicity. Comparisons of the cytotoxicities of **1** and **2** suggested that the hydroquinone skeleton of **1** conferred higher cytotoxicity than the quinoid of **2**. In addition, compound **3** is closely related to nectrianolin A [16], which is the main metabolite produced by the fungus *Nectria pseudotrichia* 120-1NP. The cytotoxic activity of **3** was compared with that of nectrianolin A (HL60: IC₅₀ = 1.7

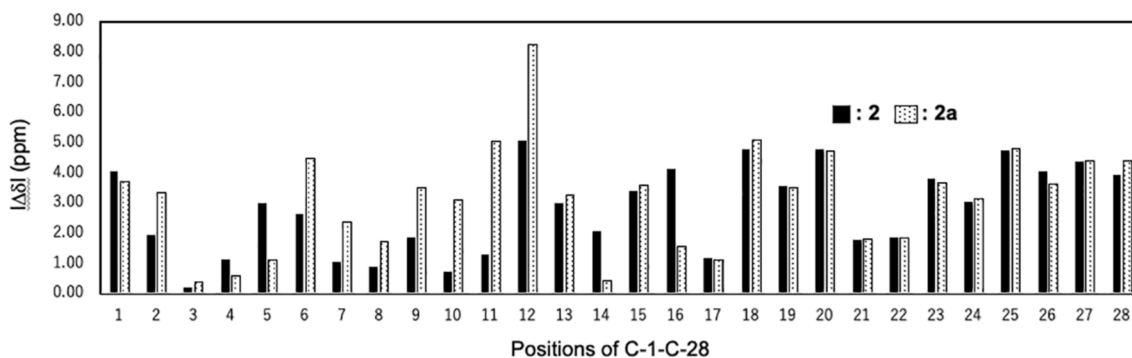


Fig. 5. Relative errors between the predicted ^{13}C NMR chemical shifts of two potential structures (2 and 2a) and recorded ^{13}C NMR of 2.

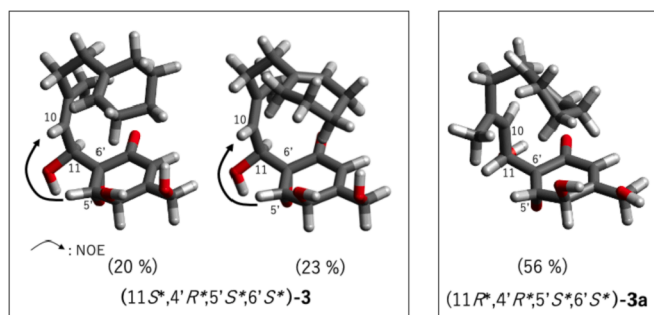


Fig. 6. Dominant rotamers around the C-6'-C-11-C-10 bonds for $(11S^*,4'R^*,5'S^*,6'S^*)$ -3 and $(11R^*,4'R^*,5'S^*,6'S^*)$ -3a and their relevant Boltzmann populations.

μM) [16]. The results showed that the trimethyl cyclohexene ring in 3 is a structural feature important for the cytotoxicity.

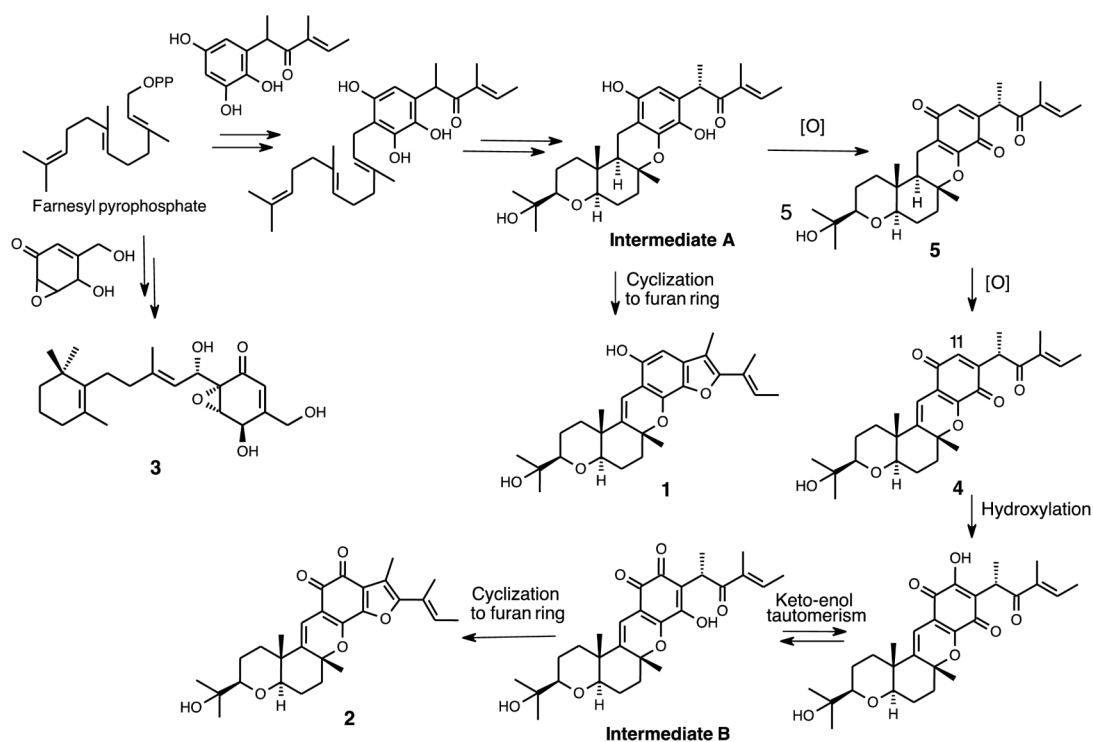
4. Conclusion

Three new and two known compounds were isolated from the coculture of the endophytic fungi, *C. rosea* B5-2 and *N. pseudotrichia* B69-1. Compounds isolated from co-culture conditions were not isolated in the monoculture condition. As mentioned earlier, nectrianolin A

Table 3

Cytotoxicity activities of compounds 1–5 against HL60.

Compounds	IC ₅₀ (μM)
1	0.47
2	0.63
3	10.16
4	0.93
5	1.61
Camptothecin	0.016



Scheme 1. Plausible biosynthetic pathway of 1, 2, 3, 4 and 5.

was isolated from the monoculture of *N. pseudotrachia* 120-1NP [16], and in relation to cochliquinones, it was reported that *Nectria* sp. Z14-w produced nectripenoids A and B [12]. *Nectria* sp. belongs to same family (Nectriaceae) to *Neonectria* sp. [19]. Therefore, co-culture method might stimulate the production of **1**, **2**, **3**, **4** and **5** by *N. pseudotrachia* B69-1. The fact that cocultivation in the present study induced the production of new fungal metabolites indicated useful strategies for triggering the production of cryptic fungal secondary metabolites and enhancing of the chemical diversity.

Compounds **1–5** were evaluated for their cytotoxic activities against HL60 cells. Among all the compounds, compound **1** showed the highest cytotoxicity against HL60 cells with an IC₅₀ value of 0.47 μM. Although the mechanism of the cytotoxicity of **1–5** remains to be determined, this study describing the structure-activity relationships of **1–5** may provide useful information for the discovery of more potent anti-tumor compounds.

Credit author statement

Ferry Ferdiansyah Sofian: Writing - original draft, Formula analysis, Separation of compounds. Takuma Suzuki: Formula analysis, Separation of compounds. Unang Supratman, Desi Harneti, Rani Maharani, Supriatno Salam, and Fajar Fauzi Abdullah: Resource, Formula analysis. Takuya Koseki: Methodology. Kurumi Tanaka, Ken-ichi Kimura: Formula analysis, biological activity. Yoshihito Shiono: Writing - original draft, Methodology.

Declaration of Competing Interest

The authors declare that there is no conflict of interest.

Acknowledgments

The authors thank Prof. Hiroyuki Konno and Prof. Takako Aboshi in Yamagata University for CD and MS experimental supports, respectively. This work was partly supported by MEXT KAKENHI Grant Number 19K05709 (Y. S) and the author (U. S) was also supported by World Class Professor Grant Number T/83/D2.3/KK.04.05/2019, Indonesia.

Appendix A. Supplementary data

Supplementary data to this article can be found online at <https://doi.org/10.1016/j.fitote.2021.105056>.

References

- [1] L. Yan, J. Zhu, X. Zhao, J. Shi, C. Jiang, D. Shao, Beneficial effects of endophytic fungi colonization on plants, *Appl. Microbiol. Biotechnol.* 103 (2019) 3327–3340.
- [2] B.S. Bamisile, C.K. Dash, K.S. Akutse, R. Keppanan, O.G. Afolabi, M. Hussain, M. Qasim, L. Wang, Prospects of endophytic fungal entomopathogens as biocontrol and plant growth promoting agents: an insight on how artificial inoculation methods affect endophytic colonization of host plants, *Microbiol. Res.* 217 (2018) 34–50.
- [3] V.J. Carrión, J. Perez-Jaramillo, V. Cordovez, V. Tracanna, M. de Hollander, D. Ruiz-Buck, L.W. Mendes, W.F.J. van Ijcken, R. Gomez-Exposito, S.S. Elsayed, P. Mohanraj, A. Arifah, J. van der Oost, J.N. Paulson, R. Mendes, G.P. van Wezel, M.H. Medema, J.M. Raaijmakers, Pathogen-induced activation of disease-suppressive functions in the endophytic root microbiome, *Science* 366 (2019) 606–612.
- [4] S. Kusari, S.P. Pandey, M. Spiteller, Untapped mutualistic paradigms linking host plant and endophytic fungal production of similar bioactive secondary metabolites, *Phytochemistry* 91 (2013) 81–87.
- [5] R. Dinesh, V. Srinivasan, T.E. Sheeja, M. Anandaraj, H. Srambikkal, Endophytic actinobacteria: diversity, secondary metabolism and mechanisms to unsilence biosynthetic gene clusters, *Crit. Rev. Microbiol.* 43 (2017) 546–566.
- [6] M. Frank, F.C. Özkaya, W.E.G. Müller, A. Hamacher, M.U. Kassack, W. Lin, Z. Liu, P. Proksch, Cryptic secondary metabolites from the sponge-associated fungus *Aspergillus ochraceus*, *Mar Drugs*. 17 (2019) 99.
- [7] U. Supratman, T. Suzuki, T. Nakamura, Y. Yokoyama, D. Harneti, R. Maharani, S. Salam, F.F. Abdullah, T. Koseki, Y. Shiono, New metabolites produced by endophyte *Clonostachys rosea* B5-2, *Nat. Prod. Res.* 27 (2019) 1–7.
- [8] K. Ueda, T. Beppu, Antibiotics in microbial coculture, *J. Antibiot.* 70 (2017) 361–365.
- [9] M.J. Frisch, G.W. Trucks, H.B. Schlegel, G.E. Scuseria, M.A. Robb, J.R. Cheeseman, G. Scalmani, V. Barone, G.A. Petersson, H. Nakatsuji, X. Li, M. Caricato, A. V. Marenich, J. Bloino, B.G. Janesko, R. Gomperts, B. Mennucci, H.P. Hratchian, J. V. Ortiz, A.F. Izmaylov, J.L. Sonnenberg, D. Williams-Young, F. Ding, F. Lipparini, F. Egidi, J. Goings, B. Peng, A. Petrone, T. Henderson, D. Ranasinghe, V. G. Zakrzewski, J. Gao, N. Rega, G. Zheng, W. Liang, M. Hada, M. Ehara, K. Toyota, R. Fukuda, J. Hasegawa, M. Ishida, T. Nakajima, Y. Honda, O. Kitao, H. Nakai, T. Vreven, K. Throssell, J.A. Montgomery Jr., J.E. Peralta, F. Ogliaro, M. J. Bearpark, J.J. Heyd, E.N. Brothers, K.N. Kudin, V.N. Staroverov, T.A. Keith, R. Kobayashi, J. Normand, K. Raghavachari, A.P. Rendell, J.C. Burant, S.S. Iyengar, J. Tomasi, M. Cossi, J.M. Millam, M. Klene, C. Adamo, R. Cammi, J.W. Ochterski, R.L. Martin, K. Morokuma, O. Farkas, J.B. Foresman, D.J. Fox, Gaussian 09, Revision D.01, Gaussian, Inc, Wallingford CT, 2009.
- [10] T.A. Halgren, Merck molecular force field, *J. Comput. Chem.* 17 (1996) 490–519.
- [11] M. Arayama, S. Uesugi, K. Tanaka, H. Maeda, T. Nehira, K. Kimura, M. Hashimoto, Homojesterones: vinylogous analogs of Jesterone from *Helminthosporium velutinum* TS28, *Tetrahedron* 72 (2016) 1031–1035.
- [12] X. Zhang, T.T. Wang, Q.L. Xu, Y. Xiong, L. Zhang, H. Han, K. Xu, W.J. Guo, Q. Xu, R.X. Tan, H.M. Ge, Genome mining and comparative biosynthesis of meroterpenoids from two phylogenetically distinct fungi, *Angew. Chem. Int. Ed. Engl.* 57 (2018) 8184–8188.
- [13] C.H. Lim, H. Miyagawa, T. Ueno, H. Takenaka, T. Tsurusima, Isolation and structure elucidation of terpenoid phytotoxins produced by the plant pathogenic fungus *Bipolaris cynodontis*, *Tennen Yuki Kagobutsu Toronkai Koen Yoshishu* 37 (1995) 325–330.
- [14] N. Koyama, T. Nagahiro, Y. Yamaguchi, R. Masuma, H. Tomoda, S. Omura, Stemphones, Novel Potentiators of Imipenem Activity against Methicillin-resistant *Staphylococcus aureus*, produced by *Aspergillus* sp. FKI-2136, *J. Antibiot.* 58 (2005) 695–703.
- [15] G.K. Poch, J.B. Gloer, Obionin A: a new polyketide metabolite from the marine fungus *Leptosphaeria obiones*, *Tetrahedron Lett.* 30 (1989) 3483–3486.
- [16] N.R. Ariefta, P. Kristiana, H.H. Nurjanto, H. Momma, E. Kwon, T. Ashitani, K. Tawarayama, T. Murayama, T. Koseki, H. Furuno, N. Usukhbayar, K. Kimura, Y. Shiono, Nectrianolins A, B, and C, new metabolites produced by endophytic fungus *Nectria pseudotrachia* 120-1NP, *Tetrahedron Lett.* 58 (2017) 4082–4086, <https://doi.org/10.1016/j.tetlet.2017.09.032>.
- [17] Y. Long, T. Tang, L.Y. Wang, B. He, K. Gao, Absolute configuration and biological activities of meroterpenoids from an endophytic fungus of *Lycium barbarum*, *J. Nat. Prod.* 82 (2019) 2229–2237.
- [18] M. Wang, Z.H. Sun, Y.C. Chen, H.X. Liu, H.H. Li, G.H. Tan, S.N. Li, X.L. Guo, W. M. Zhang, Cytotoxic cochliquinone derivatives from the endophytic fungus *Bipolaris sorokiniana* derived from *Pogostemon cablin*, *Fitoterapia* 110 (2016) 77–82.
- [19] F. Mantiri, G.J. Samuels, J.E. Rahe, B. Honda, Phylogenetic relationships in *Neonectria* species having *Cylindrocarpum* anamorphs inferred from mitochondrial ribosomal DNA sequences, *Can. J. Bot.* 79 (2001) 334–340.